Geoscientific
Model Development

Supplement of

Impact of increased resolution on Arctic Ocean simulations in Ocean Model Intercomparison Project phase 2 (OMIP-2)

Qiang Wang et al.

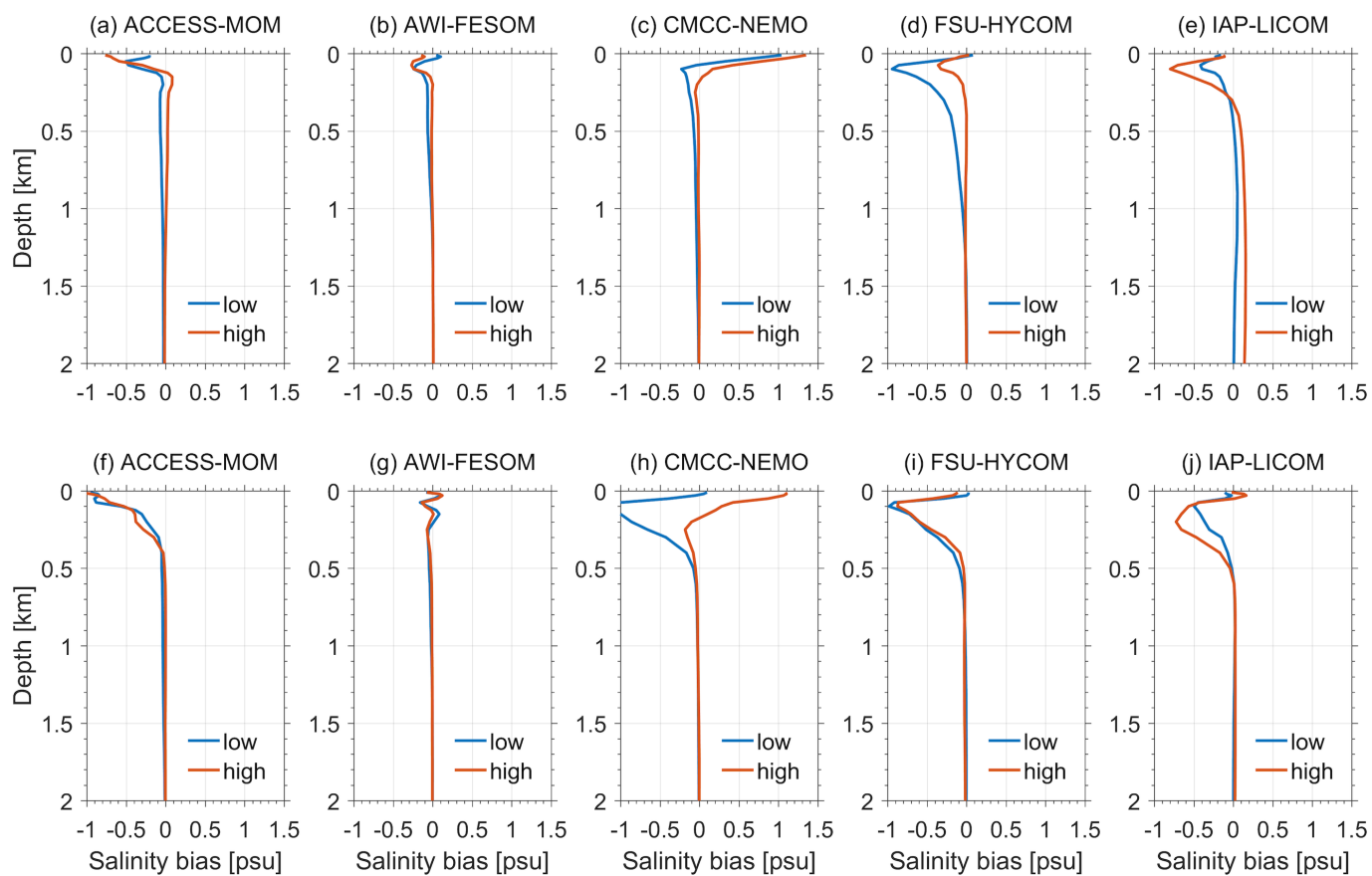*Correspondence to:* Qiang Wang (qiang.wang@awi.de)

Figure S1. Biases of basin-mean salinity for (a-e) the Eurasian Basin and (f-j) the Amerasian Basin averaged over 1971–2000. The biases are calculated relative to the PHC3 climatology.
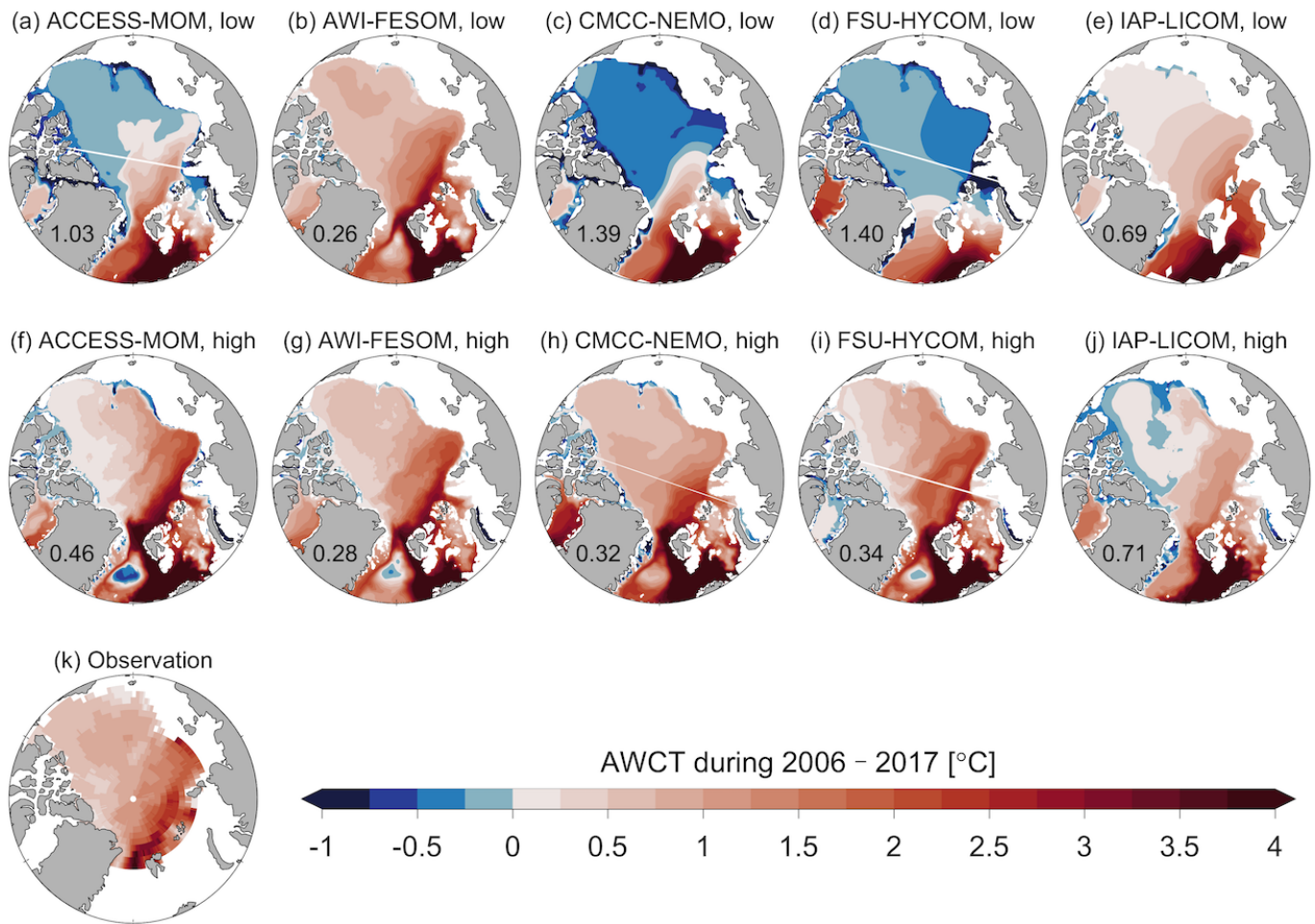
Figure S2. Simulated Atlantic Water core temperature (AWCT) averaged over 2006–2017 (a-j). (k) The AWCT for the same period based on observations (Polyakov et al., 2020). The model root-mean-square errors in the Arctic basin are displayed in each respective panel.
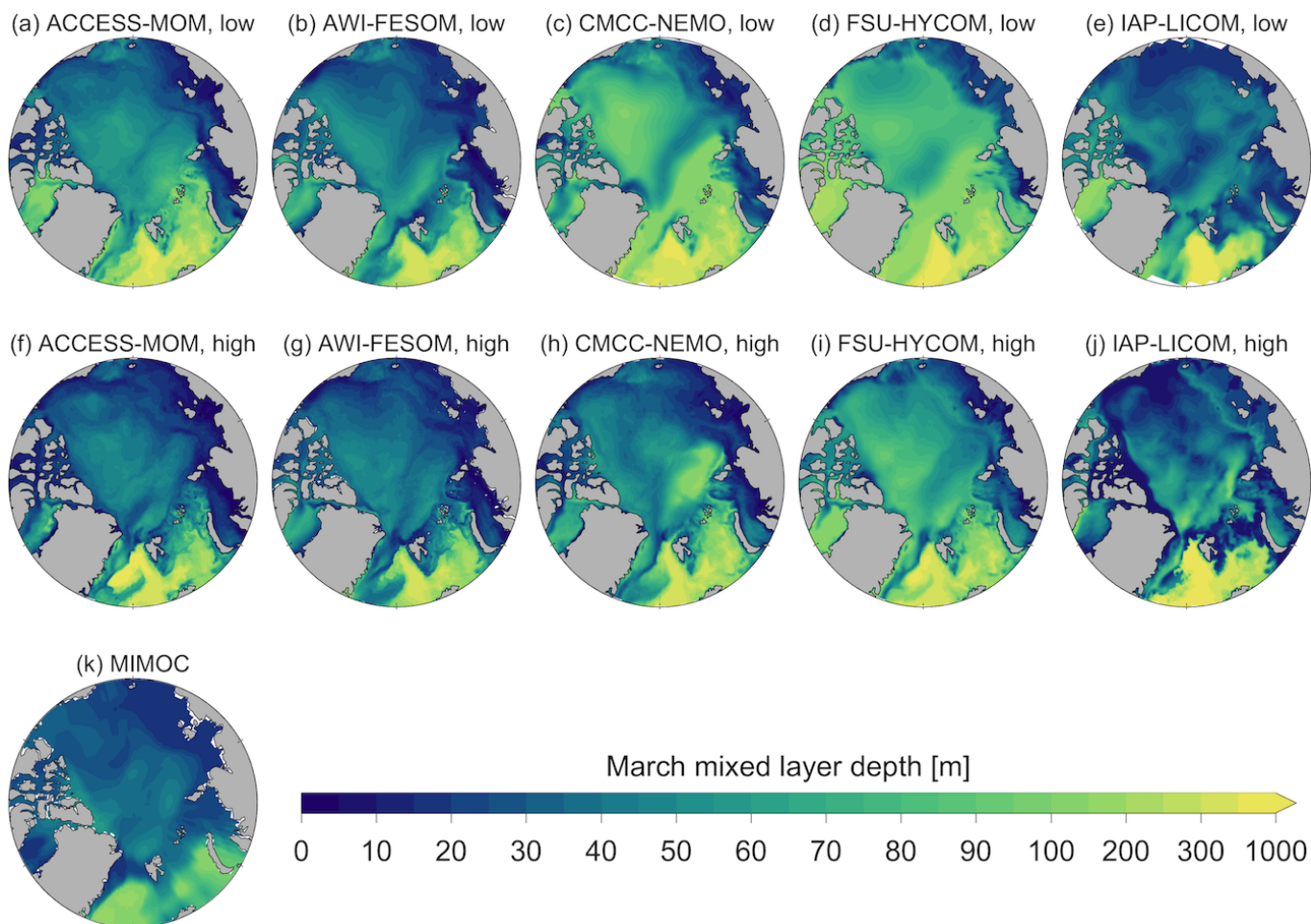
(a) ACCESS-MOM, low   (b) AWI-FESOM, low   (c) CMCC-NEMO, low   (d) FSU-HYCOM, low   (e) IAP-LICOM, low

(f) ACCESS-MOM, high   (g) AWI-FESOM, high   (h) CMCC-NEMO, high   (i) FSU-HYCOM, high   (j) IAP-LICOM, high

(k) MIMOC

March mixed layer depth [m]

0   10   20   30   40   50   60   70   80   90   100   200   300   1000

Figure S3. Mixed layer depth (MLD) in March averaged over 1971–2010. The MIMOC observational estimate (Schmidtko et al., 2013) is shown in (k). The density threshold for defining the MLD is $0.03\,\mathrm{kg/m^3}$ in this figure, different from Fig. 12 in the main text. This figure indicates that using a different MLD definition provides largely the same findings as described in the main text.
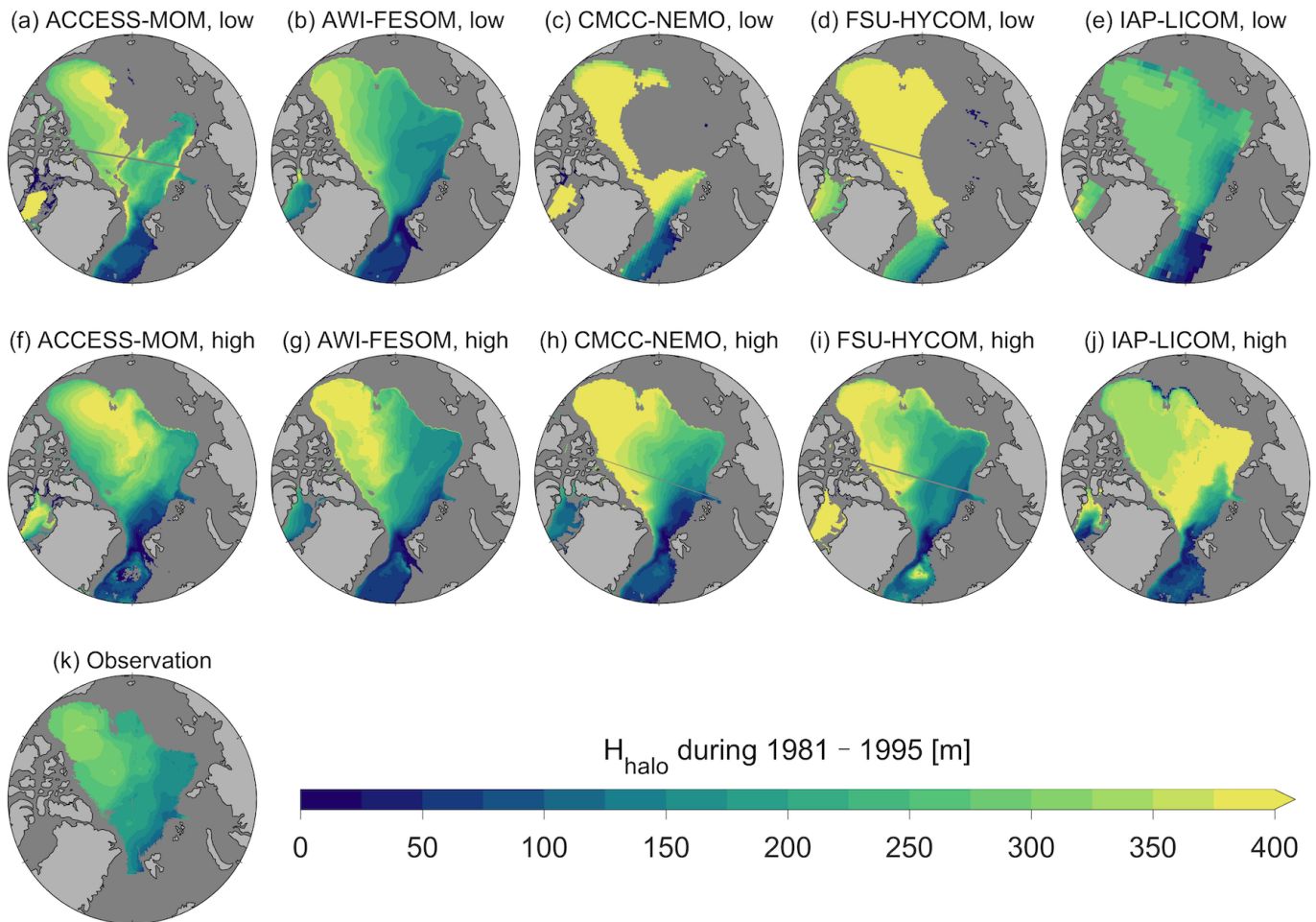
Figure S4. Cold halocline base depth averaged over 1981–1995 in low-resolution (a)-(e) and high-resolution (f)-(j) models. The observational estimate is shown in (k) (Polyakov et al., 2020).
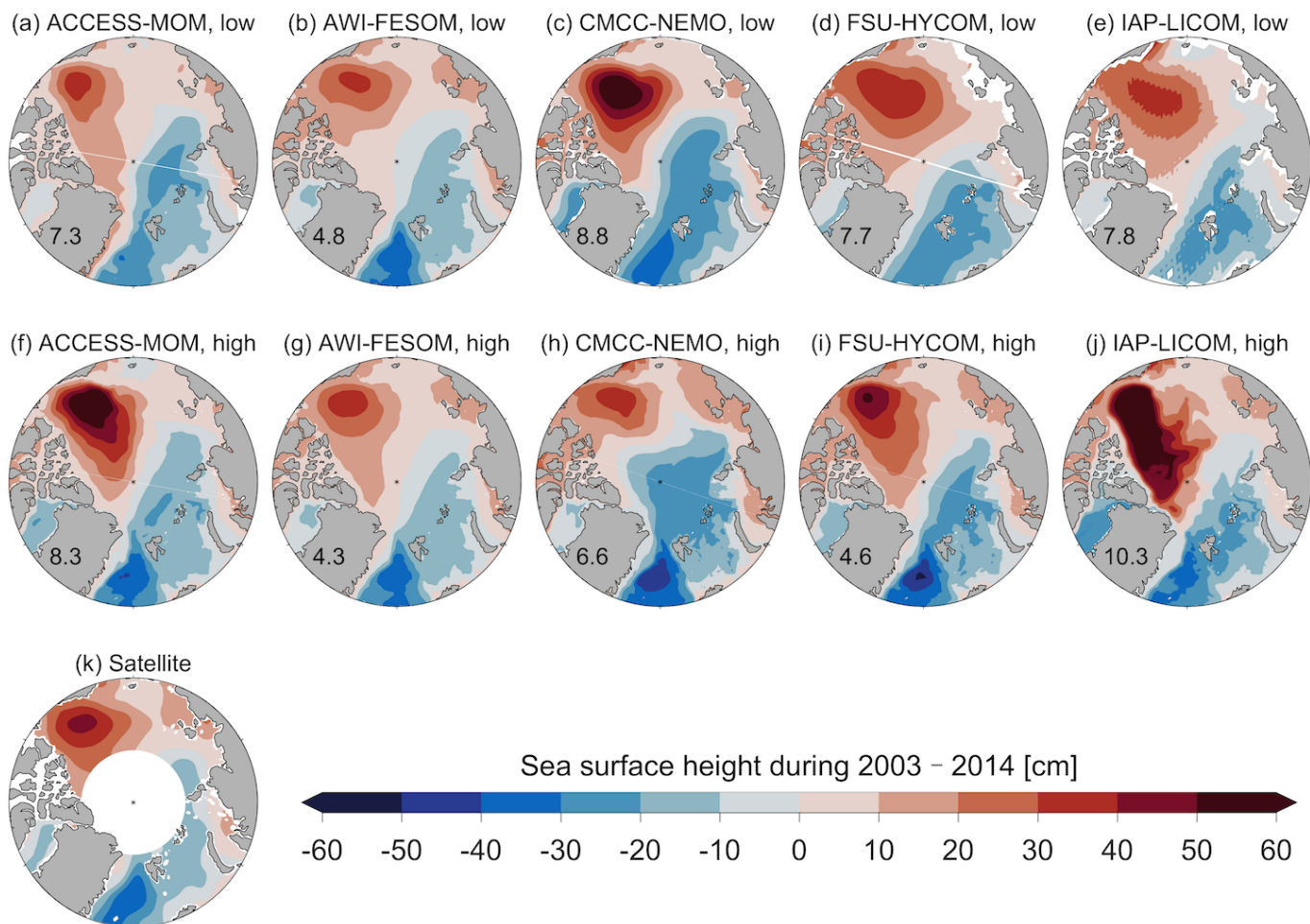
Figure S5. Sea surface height (ocean dynamic topography) averaged over 2003–2014 in low-resolution (a)-(e) and high-resolution (f)-(j) models. The satellite observation is shown in (k) (Armitage et al., 2017). The model root-mean-square errors in the Arctic basin are displayed in each respective panel.
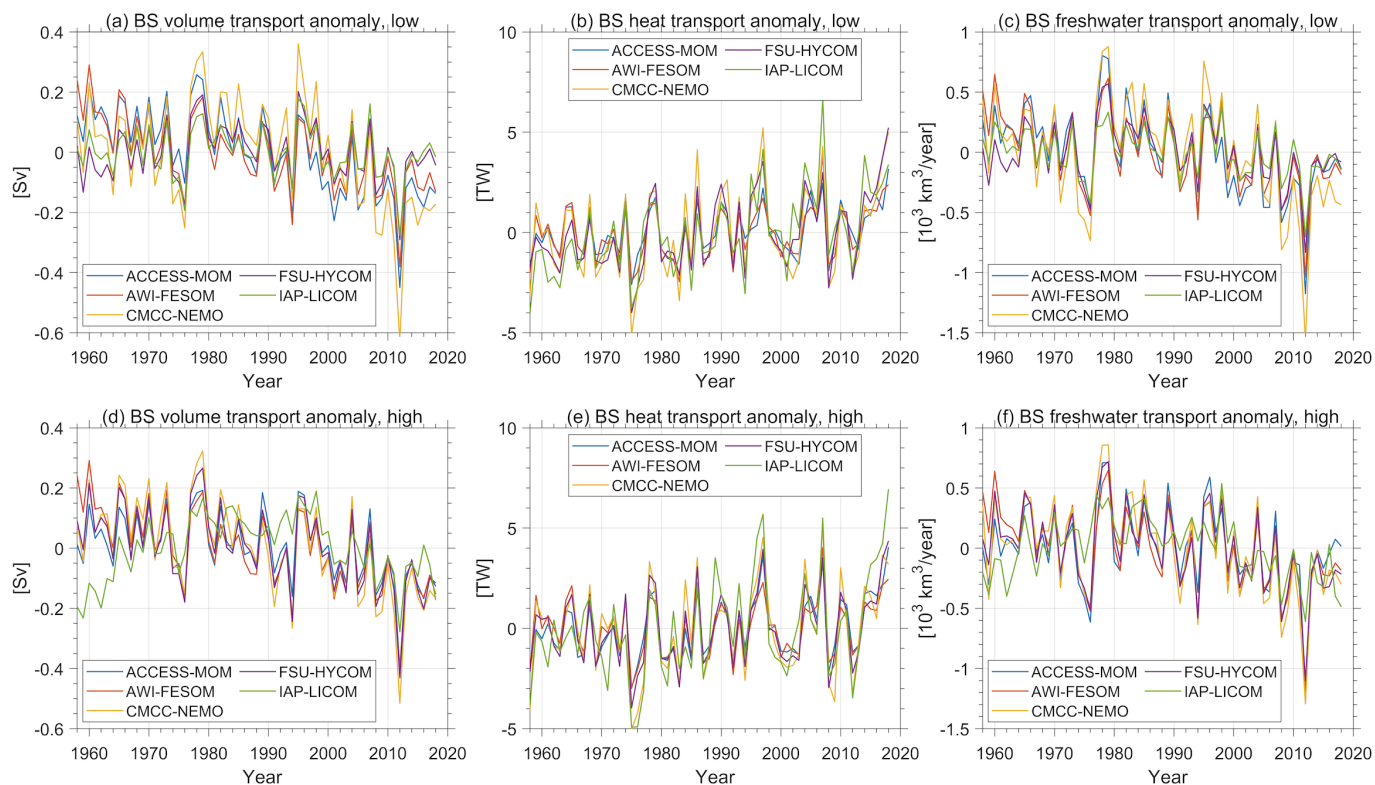
Figure S6. Anomalies of ocean (a) volume, (b) heat and (c) freshwater transports in the Bering Strait (BS) in low-resolution models. The anomalies are relative to the 1992–2008 mean. (d)(e)(f) The same as (a)(b)(c), but for high-resolution models. Heat transport is referenced to $0°C$, and freshwater transport is referenced to 34.8 psu. This figure shows the anomalies in order to better illustrate the variability; the original time series are shown in Fig. 17 in the main text.
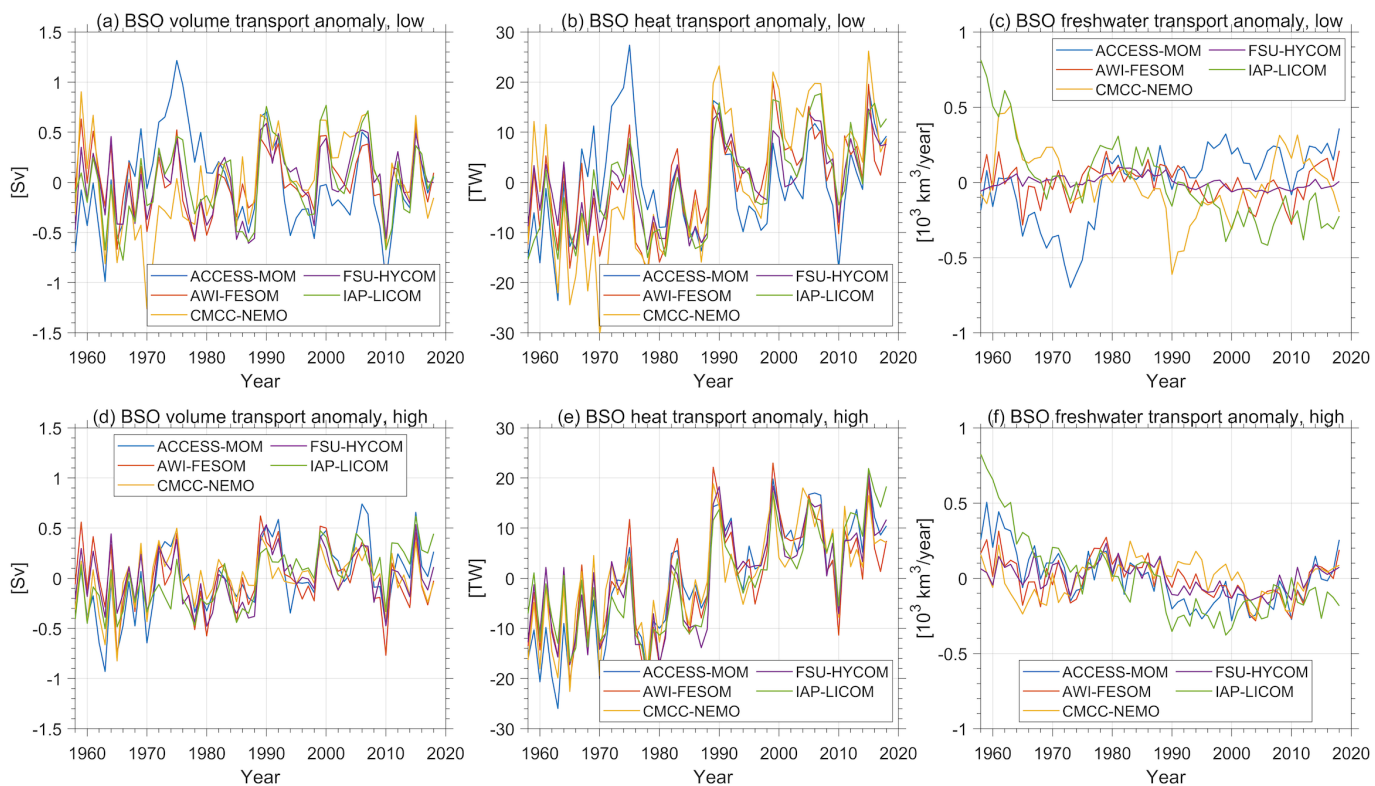
Figure S7. The same as Fig. S6, but for Barents Sea Opening (BSO). This figure shows the anomalies in order to better illustrate the variability; the original time series are shown in Fig. 18 in the main text.
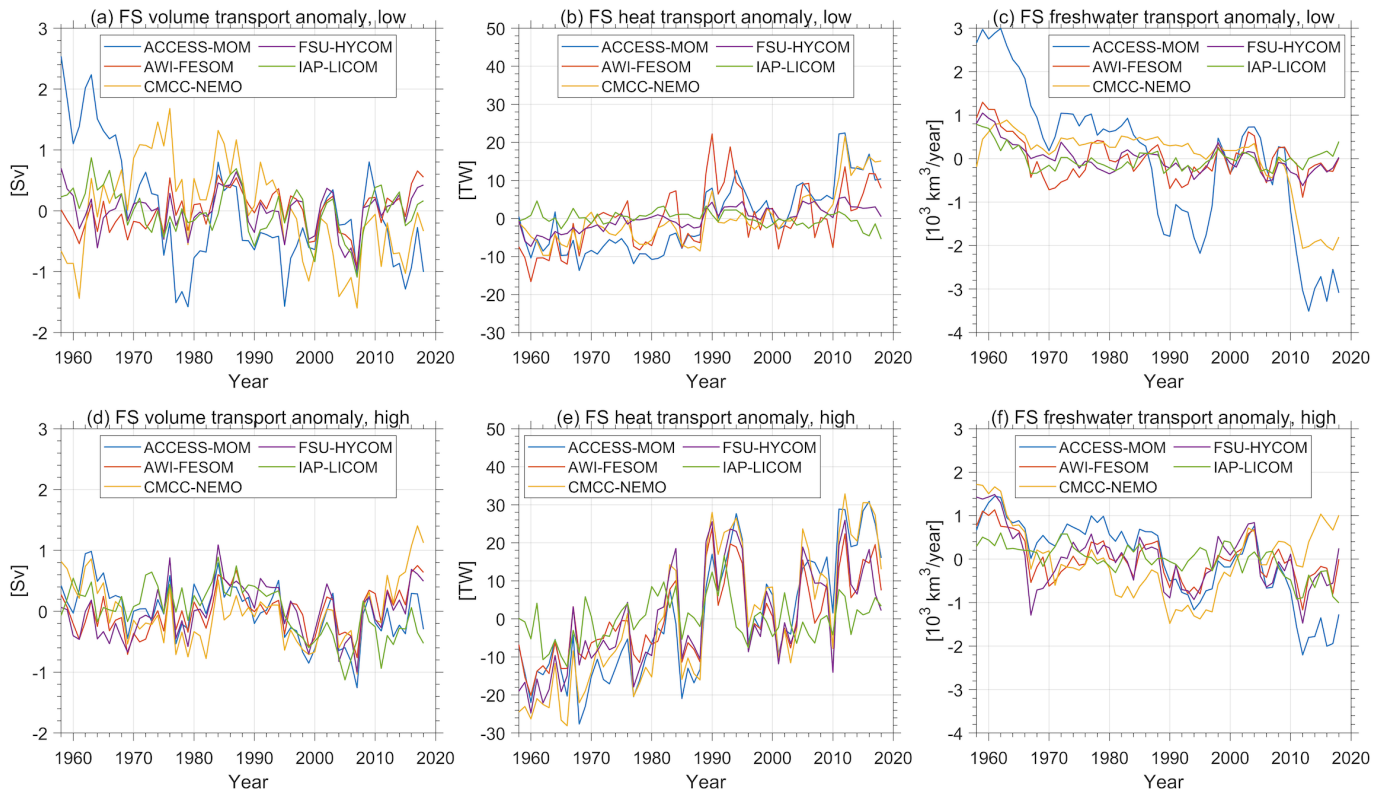
Figure S8. The same as Fig. S6, but for Fram Strait (FS). This figure shows the anomalies in order to better illustrate the variability; the original time series are shown in Fig. 19 in the main text.
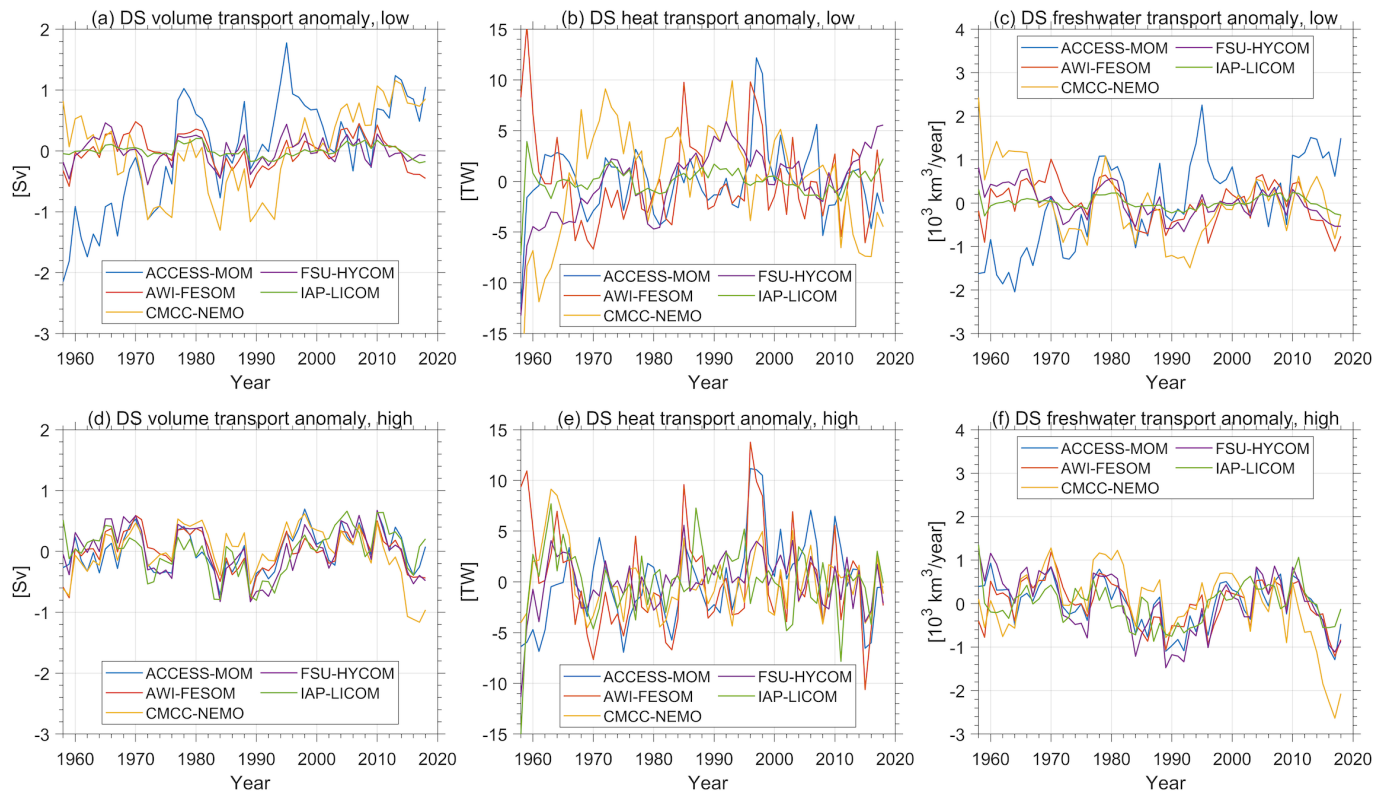
Figure S9. The same as Fig. S6, but for Davis Strait (DS). This figure shows the anomalies in order to better illustrate the variability; the original time series are shown in Fig. 20 in the main text.
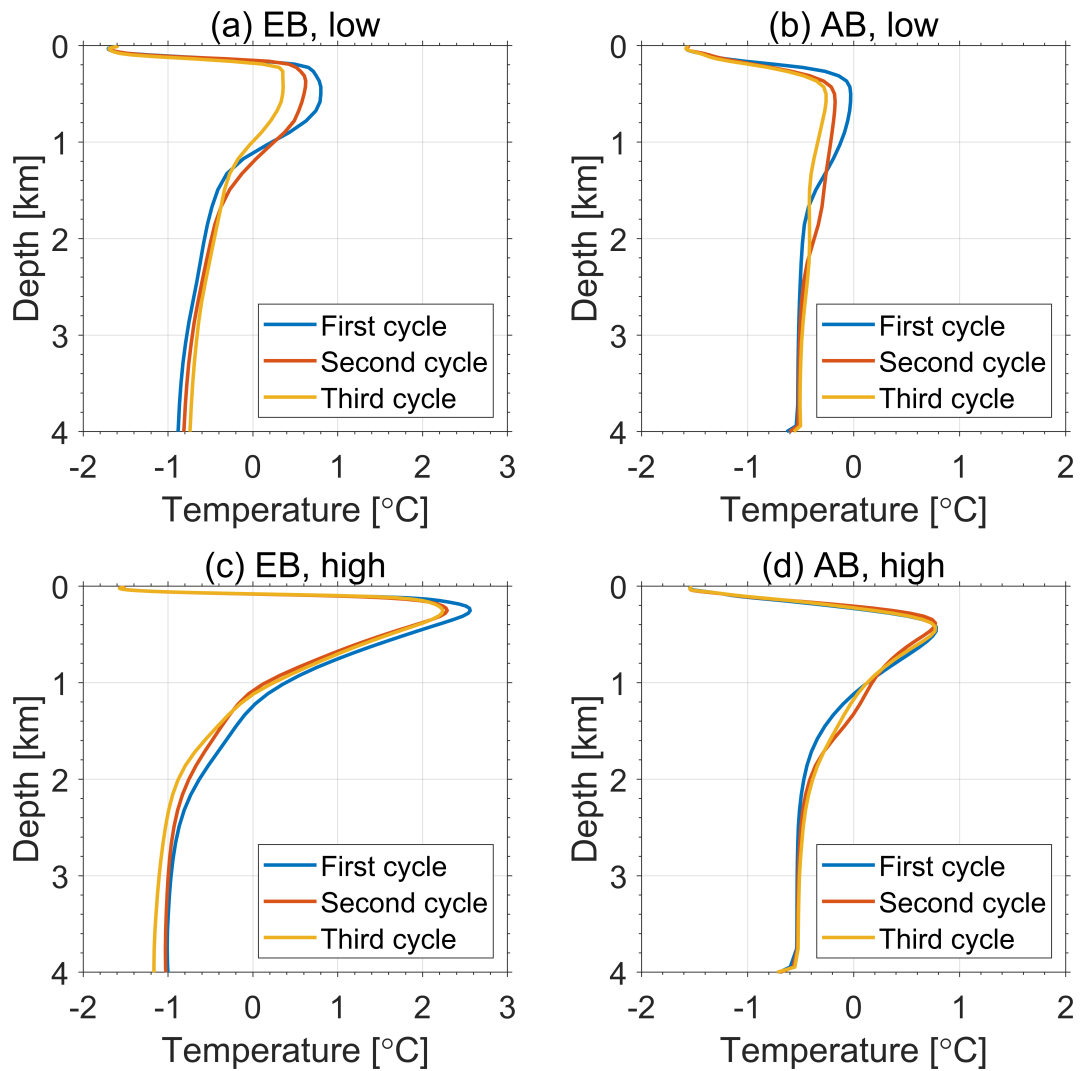
Figure S10. Temperature profiles in 2018 averaged in the Eurasian Basin (EB, left) and Amerasian Basin (AB, right) simulated in ACCESS-MOM. The upper panels display the low-resolution model results and lower panels the high-resolution model results. Results from three simulation cycles are shown.